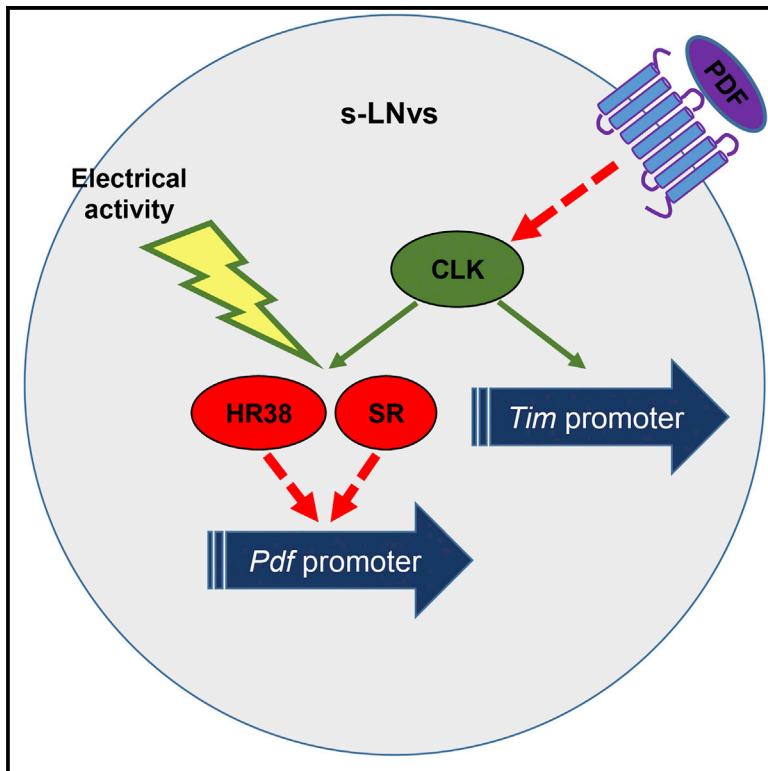# PDF Signaling Is an Integral Part of the *Drosophila* Circadian Molecular Oscillator

Graphical Abstract

Authors

Shaul Mezan, Jean Daniel Feuz,
Bart Deplancke, Sebastian Kadener

Correspondence

skadener@mail.huji.ac.il

In Brief

Using fluorescence transcriptional reporters in an ex vivo brain culture, Mezan et al. describe the existence of a reciprocal negative regulation between CLK activity and *pdf* transcription and signaling. Hence, this work uncovers an uncharacterized regulatory loop in *Drosophila* pacemaker neurons that integrates essential intra and extracellular circadian factors.

Highlights

- Monitoring circadian transcription ex vivo using fluorescent reporters

- CLK activation in the LNvs provokes downregulation in CLK activity in LNds and DNs

- Reciprocal negative regulation of CLK activity and *pdf* transcription and signaling

- PDF signaling is required for the normal oscillation pattern in CLK activity

CellPress

PDF Signaling Is an Integral Part of the *Drosophila* Circadian Molecular Oscillator

Shaul Mezan,[1] Jean Daniel Feuz,[2] Bart Deplancke,[2] and Sebastian Kadener[1,3,*]
[1]Biological Chemistry Department, Silberman Institute of Life Sciences, the Hebrew University, Jerusalem 91904, Israel
[2]Institute of Bioengineering, School of Life Sciences, EPFL, 1015 Lausanne, Switzerland
[3]Lead Contact
*Correspondence: skadener@mail.huji.ac.il
http://dx.doi.org/10.1016/j.celrep.2016.09.048

SUMMARY

Circadian clocks generate 24-hr rhythms in physiology and behavior. Despite numerous studies, it is still uncertain how circadian rhythms emerge from their molecular and neural constituents. Here, we demonstrate a tight connection between the molecular and neuronal circadian networks. Using fluorescent transcriptional reporters in a *Drosophila* ex vivo brain culture system, we identified a reciprocal negative regulation between the master circadian regulator CLK and expression of *pdf*, the main circadian neuropeptide. We show that PDF feedback is required for maintaining normal oscillation pattern in CLK-driven transcription. Interestingly, we found that CLK and neuronal firing suppresses *pdf* transcription, likely through a common pathway involving the transcription factors DHR38 and SR, establishing a direct link between electric activity and the circadian system. In sum, our work provides evidence for the existence of an uncharacterized CLK-PDF feedback loop that tightly wraps together the molecular oscillator with the circadian neuronal network in *Drosophila*.

INTRODUCTION

Behavior and physiology of most animals follow 24-hr (circadian) rhythms. These rhythms have a molecular basis and depend on self-sustaining transcriptional/post-translational feedback loops (TTFLs) (Darlington et al., 1998; Lee et al., 1998; Rosbash et al., 2007; Zheng and Sehgal, 2008). In *Drosophila*, CLK and CYC drive circadian oscillations by promoting rhythmic transcription of several key genes, including PER, TIM, and CWO, which repress CLK-CYC-mediated transcription (Allada and Chung, 2010). In addition to transcriptional control, post-transcriptional and post-translational regulatory processes play essential roles in circadian timekeeping (Kadener et al., 2009; Kim et al., 2002; Lerner et al., 2015; Lim and Allada, 2013; Sathyanarayanan et al., 2004; So and Rosbash, 1997; Yu et al., 2009).

The complexity of the circadian system extends beyond the single-cell level. In *Drosophila*, ~150 brain neurons express clock gene products. These neurons are organized into a neuronal network. They are clustered in six major subgroups: small and large ventral-lateral neurons (s-LNvs, l-LNvs, and the fifth s-LNv), dorsal-lateral neurons (LNds), and three subgroups of dorsal neurons (DNs1–3). The neuropeptide PIGMENT DISPERSING FACTOR (PDF), the main neuromodulator of the circadian neuronal network, is expressed in the LNvs. PDF is essential for normal circadian activity patterns in light:dark cycles (LD) and for persistent circadian rhythms in constant darkness (DD) (Hyun et al., 2005; Lear et al., 2005; Mertens et al., 2005; Renn et al., 1999). It exerts a widespread effect on the network (Hyun et al., 2005; Im and Taghert, 2010; Shafer et al., 2008).

Drosophila molecular studies postulate that the circadian intracellular TTFL is the main timekeeper. This assumption implies that circadian cells keep time on a cell autonomous basis. This fits well with studies performed in mammals (Nagoshi et al., 2004; Welsh et al., 2004), as well as in *Neurospora* and cyanobacteria (Brunner and Káldi, 2008; Kitayama et al., 2008). In this context, the main function of the circadian neuronal network is readjusting individual circadian oscillators, hence facilitating resonance or coherence in the network (Abraham et al., 2010; Busza et al., 2007; Depetris-Chauvin et al., 2011; Peng et al., 2003; Tang et al., 2010; Weiss et al., 2014). However, several studies provided evidence for a role of neuronal connectivity in the timekeeping process per se, in flies (Peng et al., 2003; Weiss et al., 2014) (Nitabach et al., 2002, 2005 but also see Depetris-Chauvin et al., 2011) and mammals (Bernard et al., 2007; Takahashi et al., 2010).

Nevertheless, in *Drosophila,* the extent to which the molecular and neuronal circadian networks are intertwined is still not well understood. PDF has a central role in the timekeeping process, as it coordinates phase and amplitude of molecular oscillations of downstream neurons (Collins et al., 2014; Liang et al., 2016; Lin et al., 2004; Nitabach et al., 2006; Peng et al., 2003; Seluzicki et al., 2014; Wu et al., 2008). Moreover, PDF signaling impacts the TTFL, by promoting the stabilization of the proteins TIM and PER (Li et al., 2014; Seluzicki et al., 2014). However, the effect of this regulation on CLK-driven transcription is unclear, and PDF might be merely an output of the dominant pacemaker cells (Depetris-Chauvin et al., 2011; Fernández et al., 2007; Nitabach et al., 2005; Shafer and Yao, 2014). On the other hand, CLK has a key role in development of the *pdf*-expressing neurons (Allada et al., 2003; Lerner et al., 2015; Park et al., 2000), but nothing

is known about the mechanism employed for CLK regulation over *pdf* expression. Thus, in this context, the interaction between the neuronal network and the molecular oscillator of individual neurons is far from being established.

In mammalian systems, those issues have been addressed using fluorescent reporters (Kuhlman et al., 2003; Nagoshi et al., 2004; Quintero et al., 2003). However, in *Drosophila* luciferase reporters are more commonly used (Roberts et al., 2015; Sehadova et al., 2009; Stanewsky et al., 2002). In this study, we developed and utilized fluorescent transcriptional reporters for *tim* and *pdf* in an ex vivo brain culture setup, which allows us to perturb and monitor circadian transcription with spatiotemporal precision. Using this approach, we found a reciprocal relationship between CLK activity and *pdf* transcription and signaling. Interestingly, we found that neuronal activity also modulates *pdf* transcription, likely utilizing a similar pathway as CLK, involving the transcription factors *Drosophila* hormone receptor-like 38 (DHR38) and stripe (SR). In sum, our results suggest the existence of a tight inter-cellular feedback loop, involving the transcription factor CLK and the neuropeptide PDF, that tightly wraps together the neuronal network and circadian molecular oscillators.

RESULTS

Development of a Fluorescent Circadian Transcriptional Reporter

To follow CLK-CYC driven transcription in vivo, we generated a circadian fluorescent transcriptional reporter. It contains *Drosophila* codon-optimized td-Tomato fluorophore downstream to 6.4 kb of the *timeless* control region. We fused the td-Tomato to a PEST motif and a nuclear localization signal (NLS) to produce a short-lived, nuclear-localized signal (Figures 1A and S1A). As expected, the reporter is strongly induced by addition of CLK in a system lacking this transcription factor (*Drosophila* S2 cells; Figure S1B).

We then generated transgenic flies by random insertion of the *tim*Tomato reporter. Five of the lines displayed strong oscillations in TOMATO levels across the day (Figure S1C). We choose one line (#7) with moderate fluorescent intensity, low background, and high specificity for circadian neurons for further experiments (Figure S2A). Immunostaining with anti-TIM and anti-PDF antibodies shows that the reporter is specifically co-expressed with TIM in all circadian neuronal subgroups, including the LNvs (Figures 1B and S2B). The line displays mRNA and protein oscillations in fly head extracts with similar phase and amplitude to endogenous *tim* gene products (Figures 1C, 1D, S2C, and S2D), likely due to the long maturation time of the tdTomato fluorophore (1 hr at 37°C and probably longer at 25°C). The reporter also recapitulates *timeless* expression temporally, as we detected synchronized TOMATO oscillations that peak at ZT19 across the circadian neuronal network both in light:dark (LD) as well as in free running conditions (Figures 1E, S2E, and S2F).

To determine whether the *tim*Tomato transgene can be used to report acute changes in CLK activity in vivo, we utilized the CLKGR and *Clk*SV40 transgenes. The UAS-CLKGR transgene directs the expression of a fusion between CLK and the glucocorticoid receptor ligand-binding domain. This fusion protein acts as a dominant negative of CLK (Weiss et al., 2014), but addition of the artificial glucocorticoid analog dexamethasone (Dex) activates the fusion provoking a quick and large increases in CLK-dependent transcription (Kadener et al., 2007; McDonald and Rosbash, 2001; Weiss et al., 2014). We drove expression of CLKGR with the *tim*GAL4 driver (*tim*CLKGR-*tim*Tomato flies) and observed a strong upregulation in signal from the reporter, within the circadian cells, in brain of flies incubated with Dex (Figure S2G). Our *tim*Tomato reporter also displayed a strong increase in TOMATO in flies carrying a *Clk*SV40 transgene (Figure S2H). Overall, the *tim*Tomato reporter recapitulates *timeless* spatiotemporal expression.

An Ex Vivo System for Assaying Real-Time Dynamics of CLK Transcriptional Activity

Circadian rhythms are monitored from cultured adult *Drosophila* brains using luciferase reporters (Roberts et al., 2015; Sehadova et al., 2009; Sellix et al., 2010; Stanewsky et al., 2002). To further establish the use of the brain culture system for long-term studies of the circadian network, we dissected fly brains and cultured them in LD for 5 days. We visualized VRI and PDF levels by post-culture immunostaining and found that VRI oscillations persisted in all circadian neuronal groups with similar phase, peaking at ZT15 (Figures 1F and S2I).

We utilized this brain culture in combination with our reporter to follow CLK-driven transcription immediately after induction of CLK activity in all circadian cells (using *tim*CLKGR-*tim*Tomato flies). As expected, addition of Dex strongly upregulates the reporter in all neuronal groups (Movies S1, S2, and S3). The response starts within less than 24 hr, reaching a plateau after approximately 48–60 hr (Figure S3). Our results demonstrate that dynamic changes in CLK-mediated transcription can be manipulated and simultaneously monitored ex vivo using our reporter across the circadian neuronal network.

CLK Activity in the LNvs Determines the Levels of CLK-Driven Transcription across the Circadian Neuronal Network

We followed by using our reporter in the brain culture system with the CLKGR transgene to determine the relationship between CLK-driven transcription in the LNvs and the rest of the circadian neuronal network. We generated flies expressing the UAS-CLKGR transgene under the control of the *pdf*GAL4 driver together with the reporter (*pdf*CLKR-*tim*Tomato flies). The number of *tim*Tomato positive cells was used as a proxy for signal intensity. As expected, expression of the dominant-negative protein CLKGR in the LNvs resulted in a low number of cells expressing detectable levels of the reporter at ZT19 (Figure 2A; Vehicle). We observed that a large proportion of the DNs and LNds still displayed strong TOMATO signal. Addition of Dex dramatically increased the number of cells expressing the *tim*Tomato reporter in the LNvs. Interestingly, the induction of CLK transcriptional activity in the LNvs suppressed reporter signal in the DNs and LNds (Figure 2A; Dex). The frequency plot of the number of cells expressing TOMATO illustrates this compensatory response (Figure S4A). The activation of CLKGR in the LNvs appeared to consistently inhibit *tim* transcription in the DNs and in some LNds.
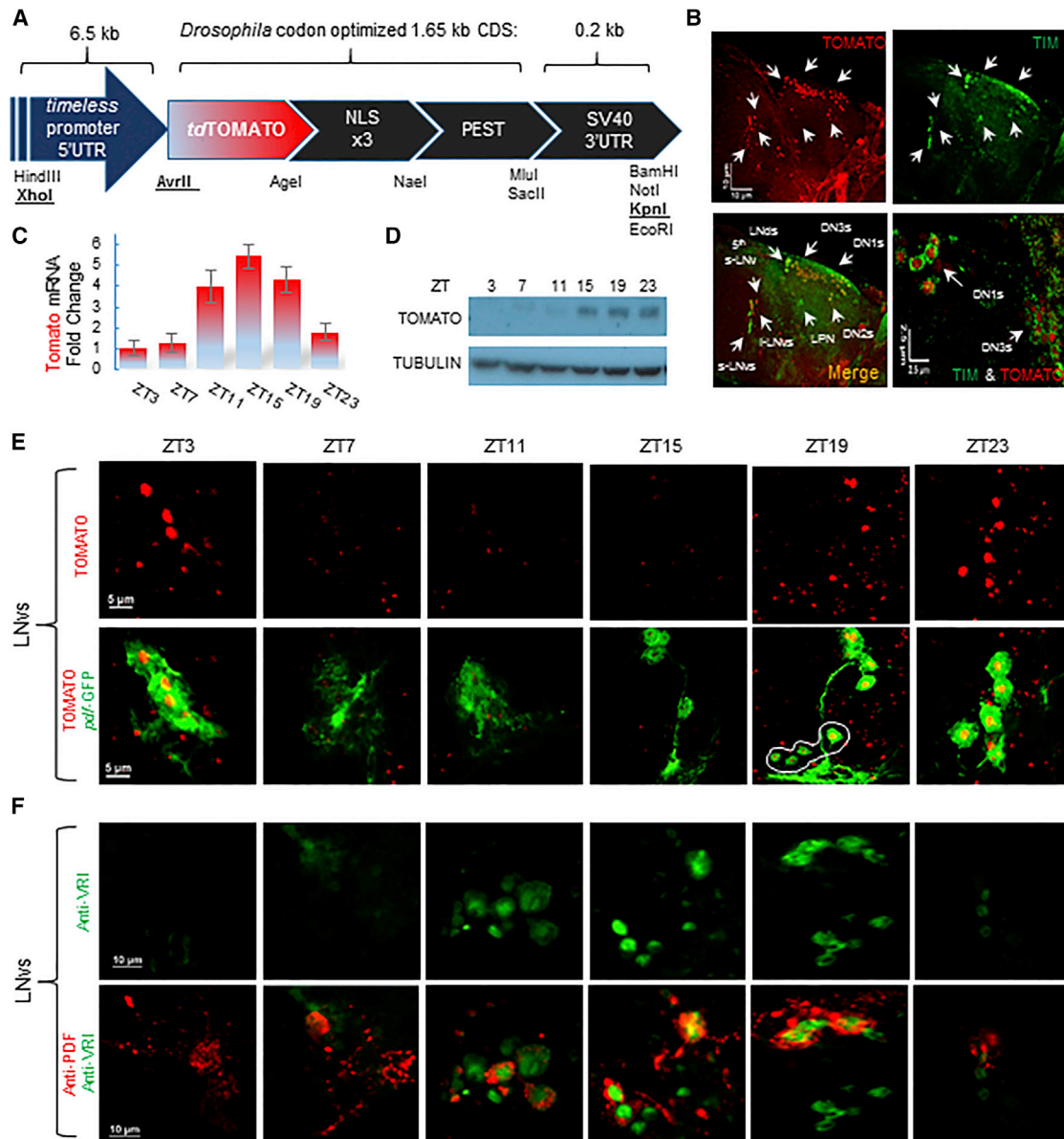
Figure 1. A Fluorescent Circadian Reporter to Assess CLK-Driven Transcription

(A) Scheme of the *tim*Tomato transcriptional reporter. Restriction sites are indicated below the scheme. NLS, nuclear localization signal; PEST, mouse ornithine decarboxylase; SV40-3′-UTR, Simian virus 3′ UTR. See also Figure S1A.

(B) The *tim*TOMATO reporter recapitulates TIM (green) spatial expression. Representative pictures from whole-mount immunohistochemistry of reporter brains stained with anti-TIM at ZT17. The nuclear TOMATO signal is surrounded by cytoplasmic TIM signal (bottom right).

(C) Daily oscillations in *Tomato* mRNA levels measured by qPCR. Error bars represent SD of three biological repeats.

(D) Western blot analysis showing the levels of TOMATO and TUBULIN in *tim*Tomato fly head across the day, performed in three biological repeats.

(E) TOMATO neuronal oscillations in the LNvs. Signal of endogenous TOMATO (red) and GFP (green) in brains of UAS-mcd8GFP; *tim*Tomato/*pdf*GAL4 flies that were entrained under 12:12 Light:Dark (LD) conditions, collected, and dissected at the indicated time point. See also Figure S2E.

(F) Oscillations of VRI in cultured brains. Dissected brains of wild-type (Canton S) flies were incubated in culture under 12:12-hr LD conditions for 5 days and then collected and stained for VRI (green) and PDF (red).

See also Figure S2I.

To determine the kinetic of this response, we monitored, by live imaging, TOMATO signal from brains of *pdf*CLKGR-*tim*Tomato flies immediately after addition of Dex to the culture (Movie S4; Figures 2A, bottom right, and S4B). We observed a quick repression in TOMATO signal in the DN1s, shortly after addition of Dex. A quick response in this cellular group is consistent with the physical interaction between s-LNvs and DN1s (Seluzicki et al., 2014). The DN3s were also strongly but slowly
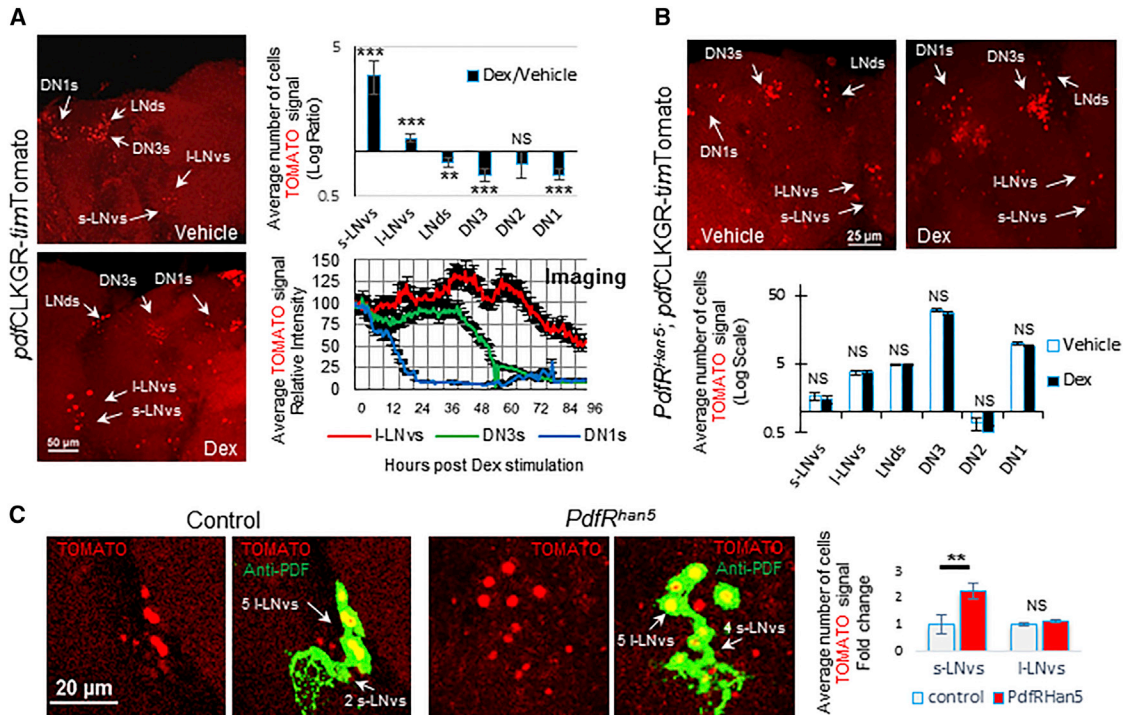
Figure 2. Activation of CLK-Driven Transcription in the LNvs Downregulates the *tim*TOMATO Reporter in Dorsal Neurons

(A) CLKGR transcriptional activity is induced in the LNvs of *Pdf*GAL4/*tim*Tomato;UAS-CLKGR (*pdf*CLKGR-*tim*Tomato) cultured brains by Dex. CLKGR activation decreases TOMATO signal in the DN1s, DN3s, and LNds at ZT19. Left: representative pictures of vehicle (top) and Dex (bottom)-treated brains. Right: quantifications of the response in different neuronal subgroups (top) and kinetic of the response monitored by time-lapse imaging (one frame/30 min) (bottom). $N_{Dex} = 71$, $N_{vehicle} = 80$ hemispheres. See also Figure S4A.

(B) Applying Dex to culture brains of *PdfR^han5*;*pdf*GAL4/*tim*Tomato;UAS-CLKGR flies (*PdfR^han5*-*pdf*CLKGR-*tim*Tomato) does not stimulate any response in the network at ZT19. Top: representative pictures of vehicle (left) and Dex (right)-treated brains. Bottom: quantification of the response. $N_{Dex} = 51$, $N_{vehicle} = 44$ hemispheres.

(C) TOMATO signal is elevated in cultured brains of *PdfR^han5*;*tim*Tomato;UAS-CLKGR (*PdfR^han5*) relative to *tim*Tomato;UAS-CLKGR brains (control). Left: representative pictures of reporter brains immunostained with anti-PDF antibody (green). A fifth l-LNvs nucleus that is PDF negative is also visible. Right: quantification of the response. n = 31, 20 hemispheres, respectively.

Statistical significance determined using two-tailed Student's t test. NS, not significant, *p < 0.05, **p < 0.01, ***p < 0.001, ****p < 0.0001. Error bars represent SEM.

affected suggesting that the effect is indirect. TOMATO signal in the l-LNvs remained high throughout this time course.

To determine whether this response depends on PDF signaling, we performed the same culture assay utilizing *pdf*CLKGR-*tim*Tomato flies that also carry a mutation in the PDF receptor (*PdfR^han5*; Hyun et al., 2005). Indeed, the presence of the *PdfR^han5* mutation eliminated the difference in TOMATO signal between vehicle-treated and Dex-treated brains in all neuronal subgroups (Figure 2B), demonstrating that this response depends on PDF signaling.

PDF Signaling Regulates Transcription Oscillations in the s-LNvs

Surprisingly, in *PdfR^han5*;*pdf*CLKGR-*tim*Tomato flies, we did not detect any difference in TOMATO signal between vehicle-treated and Dex-treated brains even in the s-LNvs and l-LNvs (Figure 2B, bottom). This strongly suggests that PDF signaling is required for the cell-autonomous increase in CLKGR-driven transcription induced by addition of Dex. In addition, we observed that introduction of the *Pdf* receptor mutation lead to a 4-fold increase in

TOMATO signal in the s-LNvs of cultured brains (Figure S4C). Importantly, the increase does not depend on the expression of CLKGR (Figure 2C), showing that PDF signaling regulates CLK-mediated transcription, at least in cultured brains. These results indicate that PDF signaling suppresses CLK-transcriptional activity in the main pacemaker neurons.

CLK Negatively Regulates *pdf* Transcription Post-development

We next decided to investigate whether CLK activity regulates *pdf* expression. Indeed, at the same culturing conditions described above, treatment of *pdf*CLKGR brains with Dex resulted in a significant elevation in PDF levels as indicated by quantification of PDF signal intensity in the LNv cell bodies and the number of PDF positive cells (Figure S5A, top right and bottom right).

To assess whether CLK regulates *pdf* at the transcriptional level, we generated transgenic flies carrying a *pdf*Tomato transcriptional reporter, which we built using the same fluorescent protein under the control of a 2.4-kb genomic region from the
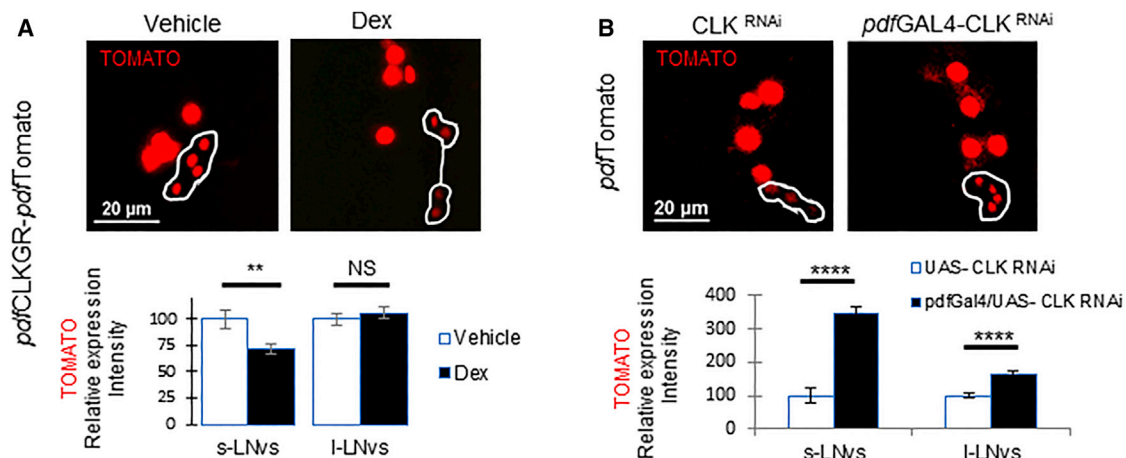
Figure 3. CLK Represses *pdf* Transcription

(A) CLKGR activation by Dex in cultured brains downregulates expression from the *pdf*Tomato (red) at ZT5. PdfGAL4; *pdf*Tomato/UAS-CLKGR (*pdf*CLKGR-*pdf*Tomato). Top: representative pictures of vehicle (left) and Dex (right)-treated brains. Bottom: quantification of the response. $N_{Dex} = 38$, $N_{vehicle} = 41$ hemispheres. See also Figure S5C.

(B) Expression of *Clk* RNAi increases *pdf* transcription (red) at ZT5. Top: representative pictures of *pdf*Tomato/UAS-CLK[RNAi] brains indicated as CLK[RNAi] (left) and *pdf*GAL4;*pdf*Tomato/UAS-CLK[RNAi] flies indicated as *pdf*GAL4-CLK[RNAi] (right). Bottom: quantification of TOMATO intensity in the LNvs. n = 24, 25 hemispheres respectively.

Statistical significance was determined using two-tailed Student's t test, NS, not significant *p < 0.05, **p < 0.01, ***p < 0.001, ****p < 0.0001. Error bars represent SEM.

pdf gene (Figure S5C; Park et al., 2000). The reporter is highly specific, thus making identification of *pdf*-expressing cells straightforward (Figure S5C, right). We generated *pdf*CLKGR flies that carry this reporter (*pdf*CLKGR-*pdf*Tomato). Despite the above-mentioned positive effect on PDF levels, activation of CLKGR by addition of Dex decreased *pdf* transcription specifically in the s-LNvs, as indicated by the intensity of TOMATO signal (Figure 3A). This result suggests that CLK activity in the LNvs inhibits *pdf* transcription. To confirm this post-developmental effect of CLK on *pdf* transcription in vivo, we knocked down *Clk* in the LNvs of *pdf*Tomato brains using the *pdf*GAL4 driver (*pdf*GAL4-*pdf*Tomato-CLK[RNAi]). In agreement with the result described above, downregulation of *Clk* in developed *pdf*-expressing cells resulted in more than 3-fold upregulation in TOMATO intensity in the s-LNvs and with a mild increase in PDF levels (Figures 3B and S5B). Overall, we conclude that CLK suppresses *pdf* transcription post-development.

DHR38 and SR Links CLK Activity to *pdf* Transcription

To determine the mechanism by which CLK regulates *pdf* expression, we identified putative regulators of *pdf* transcription using a yeast one-hybrid (Y1H) screen. For doing so, we generated five partially overlapping fragments from the 2.5-kb *pdf* promoter (Figure S6) and utilized a previously described library of 650 *Drosophila* transcription factors (Hens et al., 2011). This assay identified 27 putative regulators of *pdf* (Table 1). We then focused on candidates that are strongly enriched in the s-LNvs and known to be activated by the *Mef2* and CLK transcription factors (Abruzzi et al., 2011; Kula-Eversole et al., 2010; Nagoshi et al., 2010; Sivachenko et al., 2013). *Mef2* has been shown to mediate between CLK and the plasticity of the terminals in the *pdf*-expressing cells. We found two such candidates DHR38

and SR (Figure S6). We assessed the effect of these factors on *pdf* transcription by expressing RNAi transgenes in the *pdf*-expressing cells of flies which also carry the *pdf*Tomato reporter (*pdf*GAL4-*pdf*Tomato-RNAi). Interestingly, downregulation of *dhr38* and *sr* led to a strong upregulation of *pdf* transcription (Figures 4A and 4B), suggesting that both transcription factors inhibit *pdf* transcription. Consistently with this result, downregulation of *sr* lead to an increase in PDF levels (Figures 4B and S7C). However, downregulation of *dhr38* either in the *pdf* or *tim*-expressing cells reduced PDF levels, suggesting that this transcription factor regulates PDF expression at different levels (Figures 4A, S7A, and S7B).

Neuronal Activity Modulates *pdf* Expression

Interestingly, *dhr38* and *sr* were also identified as activity regulated genes in *Drosophila* (Fujita et al., 2013; X. Chen and M. Rosbash, personal communication) suggesting neuronal firing could regulate *pdf* levels. Thus, we determined whether *pdf* transcription is regulated by neuronal firing by using the heat-activated cation channel *dTrpA1* (Rosenzweig et al., 2005) in the *pdf*-expressing cells of flies that also carry the *pdf*Tomato reporter (*pdf*GAL4-*pdf*Tomato-TRP). DHR38 protein levels have been shown to reach a maximal expression within 2 hr of stimulation of the *dTrpA1* channel (Fujita et al., 2013). Thus, we determined the changes in TOMATO expression and PDF immunoreactivity in the LNvs of flies that were entrained at 25°C and stimulated at 33°C for 2 hr (Figure 4C). We observed that both experimental and control groups respond to the heat stimulation by downregulating TOMATO and PDF levels (Figure 4C), plausibly due to the partial overlap in expression of the endogenous *dTrpA1* channel—RNA and protein—with the PDF-expressing cells and the s-LNvs specifically (Das et al., 2016; Kula-Eversole et al.,

Table 1. Putative Regulators of *pdf* Identified by Yeast One-Hybrid Assay

	Bait Position Relative to TSS	Interacting Gene Identified
1	−2447 to −1756	CG17612
2		CG4575
3	−1967 to −1368	Abd-B
4		ecd
5		CG31835
6		CG9571
7		CG14117
8		CrebA
9	−1526 to −923	ttk
10		drm
11		crol
12		sna
13		CG4282
14	−1130 to 535	drm
15		rib
16		sd
17		Snoo
18	−690 to −1	ush
19		opa[a]
20		sr[a]
21		D1
22		woc
23		Hr38[a]
24		Jra ¦ kay
25		Rfx
26		CG18446
27		sqz[a]

27 genes identified as putative regulators of *pdf*. Bait position relative to the *pdf* promoter transcription start site (TSS) is indicated for each gene. [a]Gene that was previously identified as direct CLK targets and enriched in the LNvs. Interestingly, all four bind *pdf* most proximal bait fragment (see also Figure S6).

2010). Nevertheless, the decrease in TOMATO and PDF signal intensity, relative to the basal levels at 25°C, was significantly stronger in flies overexpressing the channel in the s-LNvs (Figure 4C), and the expression of the TRP channel strongly contributed to downregulate *pdf* expression in the s-LNvs at 33°C (Figure S7D). We conclude that neuronal activity of the LNvs suppresses *pdf* expression in the s-LNv. Our previous results strongly suggest that this effect is mediated by DHR38 and SR.

PDF Signaling Positively Modulates *pdf* Expression

Our results indicate a strong and mutual regulation between *Clk* and *pdf*. This predicts that PDF should regulate *pdf* transcription, at least indirectly. To test this, we utilize the *pdf*Tomato reporter to evaluated *pdf* expression in *PdfR^han5* mutant flies. We found that both *pdf* transcription and PDF immunostaining were strongly downregulated in *PdfR^han5* flies (Figure 5A, left and right, accordingly), suggesting that PDF signaling is necessary for continuous *pdf* expression. To determine whether continuous

activation of PDF signaling will increase *pdf* transcription, we utilized the tethered-PDF (t-PDF) technology (Choi et al., 2009, 2012). Indeed, expression of t-PDF transgene in the *pdf*-expressing cells leads to a significant increase in *pdf* transcription, compared to controls, as assessed by the *pdf*Tomato reporter (Figure 5B). Together, the results presented in this section demonstrate that PDF signaling positively modulate *pdf* transcription.

DISCUSSION

Here, we utilized an ex vivo brain culture system combined with recently developed fluorescent transcriptional reporters to analyze interactions between the neuronal network and the molecular oscillator in the *Drosophila* circadian system. We found that activation of CLK in the LNvs inhibits CLK activity in the other circadian groups. We showed that CLK and PDF regulate each other and that neural activity regulates *pdf* transcription, probably through a common pathway involving the direct CLK targets *Hr38* and *sr.* We also found that PDF signaling is required for *pdf* transcription, adding additional complexity to this cycle. Together, this study identified a tight connection between the core molecular circadian pacemaker, neuronal activity, and PDF.

We present an important technical innovation: the use of fluorescent reporters in dissected brains in culture to study circadian regulation. Our reporter system can be used to evaluate *pdf* and CLK-dependent transcription at single-cell resolution. This type of system has not been used in *Drosophila*. Using our *tim* reporter, we were able to visualize and follow dynamics in CLK activity across the circadian network. Our VRI staining demonstrated that long-term ex vivo brain culture supports coherent molecular oscillations in all neuronal groups. As reported (Ayaz et al., 2008), we also observed some degree of abnormality in PDF staining of these cultures.

Our data revealed that PDF signaling negatively regulates CLK activity in the s-LNvs (Figures 2C and S4C). The *tim*Tomato reporter is the best tool available to specifically evaluate CLK-driven transcription in the s-LNvs. As, TIM and PER levels are under strong post-transcriptional control, which can also be regulated by PDF signaling (Li et al., 2014; Seluzicki et al., 2014). The latter is analogous to the one described for Vasoactive Intestinal Polypeptide (VIP) and PER1 in the mammalian suprachiasmatic nucleus (SCN) (Maywood et al., 2006). The effect of PDF signaling on CLK-driven transcription in the s-LNvs can likely be extended to the other circadian cells (Figures 2A and 2B). However, further studies are needed to determine the mechanism of this compensatory effect. This is mainly due to the opposite effects that CLK-driven transcription has on *pdf* transcription and overall PDF levels.

The lack of ability to activate the CLKGR transgene (Figure 2B) could be due to several reasons, including: (1) the *tim* promoter is already active up to its maximal capacity; (2) CLKGR cannot be activated by the addition of Dex in the *PdfR^Han5* mutants; and (3) a combination of both options. It is also possible that PDF signaling somehow interferes with Dex induction of CLKGR, although we did not find experimental support for this possibility. Since we show that in the absence of PDF signaling there is a 4-fold increase in signal originated from the *tim*Tomato reporter
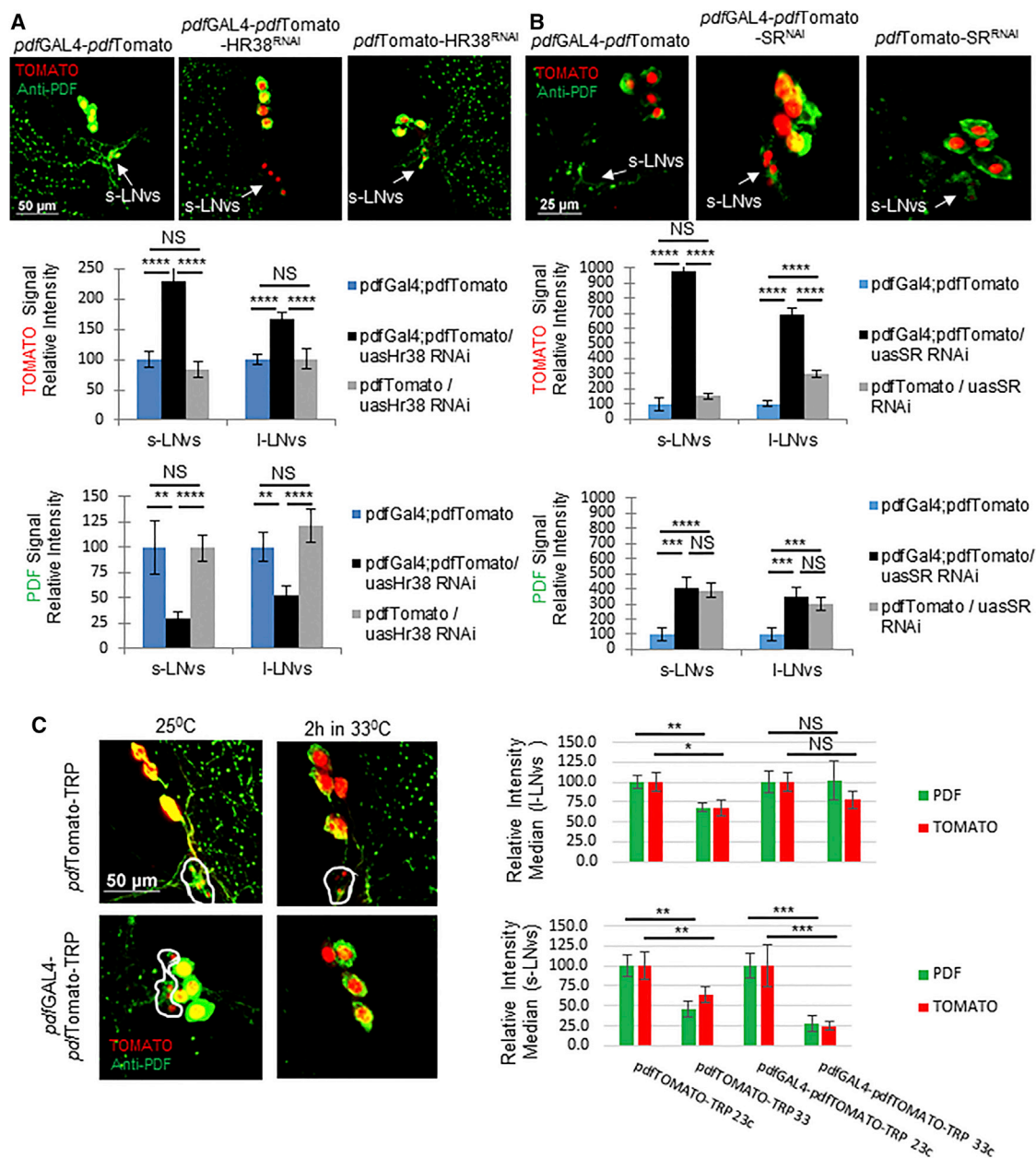
Figure 4. *pdf* Transcription Is Regulated by Electrical Activity, Likely through *Dhr38* and *sr*

Flies carrying the *pdf*GAL4;*pdf*Tomato transgenes were crossed with flies carrying the UAS-*hr38*[RNAi] (A) UAS-*sr*[RNAi] (B) and UAS-*TrpA1* (C). Brains were dissected at ZT5 and immunolabeled with anti-PDF antibody before visualization of TOMATO (red) and PDF (green).

(A and B) Top: representative pictures of the indicated genotypes from left to right: *pdf*GAL4;*pdf*Tomato, *pdf*GAL4;*pdf*Tomato/UAS-RNAi, *pdf*Tomato/UAS-RNAi. Bottom: quantification of TOMATO (upper) and PDF (lower) signal intensities in the cell body. For (A), n = 32, 33, 36 hemispheres, respectively. For (B), n = 30, 41, 37 hemispheres respectively.

(C) Left: representative pictures of the indicated genotypes: control *pdf*Tomato/UAS-TRPA1 brains (upper) and *pdf*GAL4;*pdf*Tomato/UAS-TRPA1 brains (lower), incubated for 2 hr at 25°C (left) or 33°C (right). Right: quantification of TOMATO (red) and PDF (green) signal intensities in the cell body of l-LNvs (upper) and s-LNs (lower). n = 35, 44, 53, 42 hemispheres, respectively.

See Figure S7D. Statistical significance was determined using two-tailed Student's t test, NS, not significant, *p < 0.05, **p < 0.01, ***p < 0.001, ****p < 0.0001. Error bars represent SEM.

in s-LNvs (Figure S4C) and since similar increase was observed independently of CLKGR expression (Figure 2C), we can conclude that in the absence of PDF signaling endogenous

CLK activity is higher. We speculate that the observed increase in endogenous CLK activity overrides the ability to activate CLKGR in the PdfR[Han5] flies.
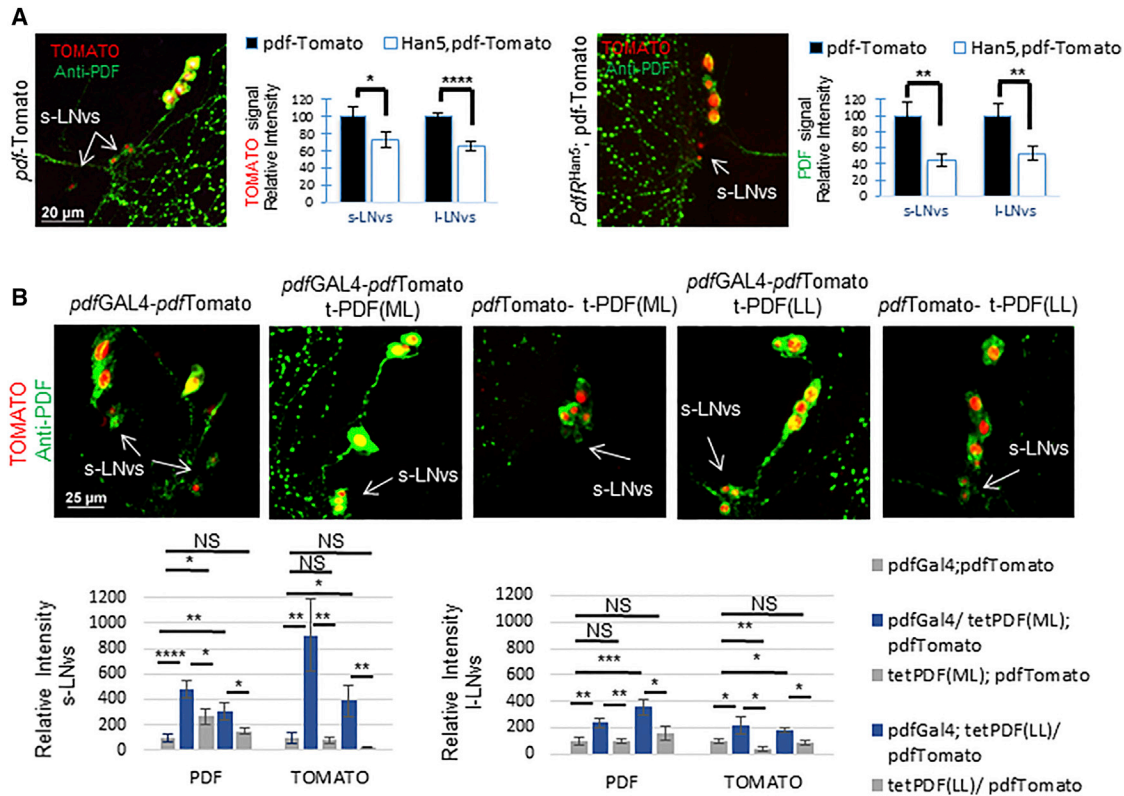
Figure 5. PDF Signaling Positively Regulates *pdf* Expression

(A) *PdfR^Han5* flies exhibit reduced levels of *pdf* transcription and PDF neuropeptide. Representative pictures of a fly brain carrying the *pdf*Tomato transgene (left) or with mutation in PDFR (*PdfR^han5*; *pdf*Tomato) (right). Reporter brains were dissected at ZT5, immunolabeled for PDF, and visualized for TOMATO (red) and PDF (green). Quantification of TOMATO (left) and PDF (right) intensities in the LNvs cell body of the whole sampled population are shown (n = 30, 38 hemispheres respectively).

(B) Flies expressing the tethered-PDF transgenes under the control the *pdf*GAL4 driver exhibit elevated levels of *pdf* transcription. *Pdf*GAL4;*pdf*-Tomato flies were crossed with UAS-tethered-PDF flies carrying short (ML) or long poly-linker (LL). Brains were dissected at ZT5, immunolabeled with anti-PDF antibody, and visualized for TOMATO (red) and PDF (green). Shown (top) are representative pictures of fly brain carrying the following genotypes (left to right): *pdf*GAL4;*pdf*Tomato, *pdf*GAL4/UAS-tet-PDF(ML);*pdf*Tomato, UAS-tet-PDF(ML);*pdf*Tomato, *pdf*GAL4;*pdf*Tomato/UAS-tet-PDF(LL), *pdf*Tomato/UAS-tet-PDF(LL). Bottom: quantification of TOMATO and PDF in the s-LNvs (left) and l-LNvs (right). n = 23, 28, 24, 25, 20 hemispheres, respectively.

Statistical significance was determined using one-tailed Student's t test. NS, not significant, *p < 0.05, **p < 0.01, ***p < 0.001, ****p < 0.0001. Error bars represent SEM.

Previous studies support the notion that CLK positively regulate the development of the *pdf* cells (Allada et al., 2003; Lerner et al., 2015; Park et al., 2000; Zhao et al., 2003). However, those studies rely on the broad expression of CLK protein. Here, we show that specific induction of CLK activity in the adult main pacemaker cells, as well as silencing CLK post-development of the *pdf* cells using the *pdf*GAL4 driver, result in repression of *pdf* transcription (Figure 6, model). This suggests opposite effects of CLK on *pdf* transcription either pre and post-development of the LNvs or within and outside the LNvs. As PDF signaling positively regulates *pdf* expression, the continuous expression of *pdf* by the LNvs is a consequence of a balance between CLK and PDF activities. Neuronal electrical activity might have a crucial role in this balance, as it can suppresses *pdf* transcription in the main pacemaker cells through *Hr38* and *sr*. The effect of CLK on *pdf* seems to also involve those factors that are direct CLK and MEF2 transcriptional targets (Abruzzi et al., 2011; Sivachenko et al., 2013) and are in the LNvs (Kula-Eversole

et al., 2010) and represses *pdf* transcription (Figure 6, model: red inhibitory arrow).

Although CLK, HR38, SR, and neuronal activity downregulate *pdf* transcription, their effects on PDF neuropeptide levels are intriguing. Knockdown of *hr38* (Figure 4A) and activation of CLKGR (Figures 3A and S5A) yielded opposite effects on the *pdf*Tomato reporter and PDF levels (up and down or down and up, respectively). This suggests that *hr38* is involved in the regulation of *pdf* by CLK but also that there might be a more complex post-translational effects on PDF. However, neural stimulation downregulates both *pdf* transcription and protein levels, reinforcing the idea of additional regulatory factors and possibly post-translational control over PDF expression/processing/secretion. Hence, our model predicts that both neuronal firing and CLK activity are indirectly regulating *pdf* transcription, not only through promoting activities of targets genes such as *dhr38* and *sr*, but also through the post-translational control over PDF (Sivachenko et al., 2013) since, as we show here,
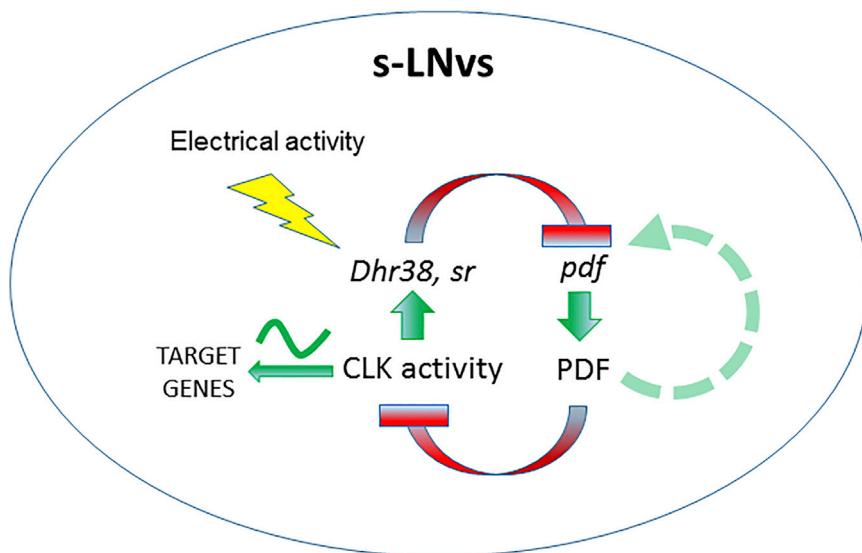
Figure 6. A Model for the Integration of PDF in the Molecular Clockwork

CLK transcriptional activity and neuronal activity indirectly regulates *pdf* levels (red inhibitory arrow) likely through a common pathway involving *hr38* and *sr* (green arrow). PDF feedbacks into the s-LNvs to resist its own inhibition by suppressing CLK activity (red inhibitory arrow) and inducing its own transcription (dotted green arrow). The model predicts that post-translational control over PDF expression/processing/secretion regulates *pdf* transcription.

PDF feeds back to regulate *pdf* transcription (model, green dotted arrow). This positive auto-regulation introduces complexity to the CLK-PDF feedback loop, and it is in agreement with a previously proposed model for PDF auto-receptor signaling in the LNvs (Choi et al., 2012). This intriguing feature of the loop should be addressed in future studies in order to extend our understanding of how post-translational mechanisms for PDF regulation affect its own transcription. The regulation of PDF signaling on *pdf* transcription can be also predicted from the strong and mutual regulation between *Clk* and *pdf*; however, we favor a more direct effect of PDF signaling on *pdf* transcription (model, green dotted arrow).

We have identified other putative regulators of *pdf* (Table 1). Their influence on *pdf* transcription remains to be determined. Interestingly, the transcription factor TTK is expressed in all TIM positive circadian neurons except the LNvs (Nagoshi et al., 2010), suggesting it might be an important endogenous regulator of *pdf* spatial expression.

PDF signaling was shown to be required for normal pattern of oscillations in CLK-driven transcription under constant darkness (Peng et al., 2003). Based on the upregulation of *tim*Tomato in PDFR mutant, we postulate that in the pacemaker cells PDF feedback is required for normal pattern of oscillations in CLK-driven transcription under light:dark cycles (Figure 6, model: inhibitory red arrow). Since ZT19 is the peak of TOMATO expression in the s-LNvs (Figure 1E, white circle), upregulation at this ZT cannot be a consequence of a phase shift; thus, it must reflect an increase in the amplitude of TOMATO oscillation. This demonstrate that in the absence of PDF signaling, the LNvs lose control of their own circadian molecular clockwork (Collins et al., 2014; Peng et al., 2003), likely because it is overridden by signals from the LNds and/or the DNs (Weiss et al., 2014; Yao and Shafer, 2014).

In sum, our findings challenge the notion that PDF is a merely output of the circadian system. Indeed, we demonstrate the existence of an uncharacterized and essential CLK-PDF-CLK regulatory loop in the LNvs that integrates PDF signaling into the single-cell molecular oscillator. The question of whether PDF feeds back to the same cells that secrete it within the subgroup of s-LNvs or whether its role as a communication agent is also applied within this subgroup remains to be answered in order to determine the final impact of this loop on the concept of cellular autonomy in the fly brain.

EXPERIMENTAL PROCEDURES

Cloning of Reporter Constructs and DNA Baits of the *pdf* Promoter

To generate the *tim*Tomato reporter construct, a *Drosophila* codon optimized TdTomato-NLSx3-PEST coding sequence was fused with a SV40 3′ UTR in a pCaSpeR4 vector downstream to a 6.4-kb DNA fragment containing the promoter and 5′ UTR stretching into to the second exon ATG of the *timeless* gene. To generate the *pdf*Tomato reporter, we utilized a similar approach but using a previously 2.45-kb fragment containing the genomic region upstream to the *pdf* gene transcription start site inserted in a pattB based vector. To generate DNA baits of the *pdf* promoter for *Drosophila* transcription factor screen (Y1H), we used a carrier vector containing the 2.45-kb promoter of the *pdf* gene as a template to generate five overlapping PCR fragments approximately 600 bp long (see the Supplemental Experimental Procedures).

Fly Strains

The reporter transgenic fly lines were generated by BestGene using the P-element-mediated germline transformation for *tim* reporter and PhiC31 integrase method into the pattP2 site for *pdf* reporter.

*Tim*GAL4, *pdf*GAL4,pdfR[Han5]; UAS-CLKGR; UAS-*Dcr2, Hr38*[RNAi], *sr* [RNAi], *Clk* [RNAi],UAS-*t-PDF*, UAS-TrpA1, and *Clk*SV40 fly lines were previously described (Choi et al., 2009, 2012; Dietzl et al., 2007; Hyun et al., 2005; Kaneko and Hall, 2000; Lerner et al., 2015; Perkins et al., 2015; Renn et al., 1999; Sivachenko et al., 2013; Weiss et al., 2014).

Drosophila Adult Brain Culture

Flies were dissected (leaving trachea and imaginal discs) in 1 × PBS on a clean surface at room temperature. Each brain was immediately placed in a separate well of a 96-well plate containing 150 μl *Drosophila* Shield and Sang M3 insect medium (10% FBS, insulin [10 μg/mL], and a 1:100 dilution of antibiotic solution). For activation of CLKGR in culture, the medium was prepared with a supplement of 10 mg/mL dexamethasone (D4902; Sigma), kept in 100% ethanol, and diluted 1:500 (Dex) or with a 1:500 dilution of 100% EtOH only (vehicle). Plates were incubated at 25°C for 96 hr under LD conditions.

Post-culture Procedure

Brains were taken out from the well, cleaned in ice-cold 1 × PBS, and then fixed with 4% paraformaldehyde (PFA) for 20 min at room temperature. Brains were then washed with ice-cold 1 × PBS before downstream application (visualization or immunolabeling) (see the Supplemental Experimental Procedures).

Live Imaging

Dissected brains were completely cleaned from trachea to avoid floating of the sample. Brains were then placed on a 12-μm cell-culture insert (Millipore) inside a 35-mm culturing dish containing 800 μl of culture medium as previously described (Ayaz et al., 2008) and entrained for 24 hr at 25°C in LD. Medium was supplemented with Dex or vehicle before time-lapse imaging was performed (one frame/30 or 40 min).

Confocal Microscopy

NIKON eclipse *Ti* confocal microscope was used to perform time-lapse imaging (Olympus ×20 super Plan Flour, 0.5 numerical aperture [NA], long distance 8,200 mm, air lens) and visualization (Olympus ×40 Plan Fluor 1.3 NA, 240 mm, ×60 Plan Apo 0.9 NA, 150 mm, oil lenses) of fluorescence.

Images Analysis and Statistics

For relative intensity quantification, background was manually determined and subtracted. Both the sum and the average signal intensity of an auto or manually detected ROIs were calculated. Signal was summed across all confocal planes surrounding the neuronal cell bodies belong to a certain sub-neuronal group in the brain. The average signal of the whole population of samples was then calculated, and statistical significance was determined. For cell-number-based quantification, microscope settings were set as permissive for weak signal (high excitation energy and low detection threshold). The number of cells in a certain neuronal group was determined based on the existence of a positive (weak or strong) TOMATO or PDF signal. TOMATO signal in the s-LNvs of reporter brains was quantified from brains over-stained for PDF and by evaluation of anatomical location. Significance was than determined using a two-tailed Student's t test.

Transfection in S2 Cells

S2 cells were maintained using standard procedures and transfected using 1.5 μl Trans-IT insect transfection reagent (Mirus). The *tim*Tomato and *tim*YFP (Lerner et al., 2015) were transfected in equal molarity (400 and 200 ng, respectively) with 100 ng pActin-CLKV5 or pMT-*Clk*SV40. DNA was adjusted to 0.5 μg with pBluescript. 12 hr post-transfection, Cu^{+2} was added to a final concentration of 1 mM. 48 hr post-induction, cells were washed and imaged.

Yeast One Hybrid

The yeast one-hybrid screens were conducted as described in Hens et al. (2011) and further detailed in Hens et al. (2012).

SUPPLEMENTAL INFORMATION

Supplemental Information includes Supplemental Experimental Procedures, seven figures, and four movies and can be found with this article online at http://dx.doi.org/10.1016/j.celrep.2016.09.048.

AUTHOR CONTRIBUTIONS

S.M. and S.K. conceived the experiments and wrote the manuscript. S.K. supervised the work. S.M. designed and performed the experiments and analyzed the data. J.D.F. and B.D. performed the Y1H screen.

ACKNOWLEDGMENTS

REFERENCES

Abraham, U., Granada, A.E., Westermark, P.O., Heine, M., Kramer, A., and Herzel, H. (2010). Coupling governs entrainment range of circadian clocks. Mol. Syst. Biol. *6*, 438.

Abruzzi, K.C., Rodriguez, J., Menet, J.S., Desrochers, J., Zadina, A., Luo, W., Tkachev, S., and Rosbash, M. (2011). Drosophila CLOCK target gene characterization: implications for circadian tissue-specific gene expression. Genes Dev. *25*, 2374–2386.

Allada, R., and Chung, B.Y. (2010). Circadian organization of behavior and physiology in Drosophila. Annu. Rev. Physiol. *72*, 605–624.

Allada, R., Kadener, S., Nandakumar, N., and Rosbash, M. (2003). A recessive mutant of Drosophila Clock reveals a role in circadian rhythm amplitude. EMBO J. *22*, 3367–3375.

Ayaz, D., Leyssen, M., Koch, M., Yan, J., Srahna, M., Sheeba, V., Fogle, K.J., Holmes, T.C., and Hassan, B.A. (2008). Axonal injury and regeneration in the adult brain of Drosophila. J. Neurosci. *28*, 6010–6021.

Bernard, S., Gonze, D., Čajavec, B., Herzel, H., and Kramer, A. (2007). Synchronization-induced rhythmicity of circadian oscillators in the suprachiasmatic nucleus. PLoS Comput. Biol. *3*, e68.

Brunner, M., and Káldi, K. (2008). Interlocked feedback loops of the circadian clock of Neurospora crassa. Mol. Microbiol. *68*, 255–262.

Busza, A., Murad, A., and Emery, P. (2007). Interactions between circadian neurons control temperature synchronization of Drosophila behavior. J. Neurosci. *27*, 10722–10733.

Choi, C., Fortin, J.P., McCarthy, Ev., Oksman, L., Kopin, A.S., and Nitabach, M.N. (2009). Cellular dissection of circadian peptide signals with genetically encoded membrane-tethered ligands. Curr. Biol. *19*, 1167–1175.

Choi, C., Cao, G., Tanenhaus, A.K., McCarthy, E.V., Jung, M., Schleyer, W., Shang, Y., Rosbash, M., Yin, J.C.P., and Nitabach, M.N. (2012). Autoreceptor control of peptide/neurotransmitter corelease from PDF neurons determines allocation of circadian activity in drosophila. Cell Rep. *2*, 332–344.

Collins, B., Kaplan, H.S., Cavey, M., Lelito, K.R., Bahle, A.H., Zhu, Z., Macara, A.M., Roman, G., Shafer, O.T., and Blau, J. (2014). Differentially timed extracellular signals synchronize pacemaker neuron clocks. PLoS Biol. *12*, e1001959.

Darlington, T.K., Wager-Smith, K., Ceriani, M.F., Staknis, D., Gekakis, N., Steeves, T.D., Weitz, C.J., Takahashi, J.S., and Kay, S.A. (1998). Closing the circadian loop: CLOCK-induced transcription of its own inhibitors per and tim. Science *280*, 1599–1603.

Das, A., Holmes, T.C., and Sheeba, V. (2016). dTRPA1 in Non-circadian Neurons Modulates Temperature-dependent Rhythmic Activity in Drosophila melanogaster. J. Biol. Rhythms *31*, 272–288.

Depetris-Chauvin, A., Berni, J., Aranovich, E.J., Muraro, N.I., Beckwith, E.J., and Ceriani, M.F. (2011). Adult-specific electrical silencing of pacemaker neurons uncouples molecular clock from circadian outputs. Curr. Biol. *21*, 1783–1793.

Dietzl, G., Chen, D., Schnorrer, F., Su, K.-C., Barinova, Y., Fellner, M., Gasser, B., Kinsey, K., Oppel, S., Scheiblauer, S., et al. (2007). A genome-wide transgenic RNAi library for conditional gene inactivation in Drosophila. Nature *448*, 151–156.

Fernández, M.P., Chu, J., Villella, A., Atkinson, N., Kay, S.A., and Ceriani, M.F. (2007). Impaired clock output by altered connectivity in the circadian network. Proc. Natl. Acad. Sci. USA *104*, 5650–5655.

Fujita, N., Nagata, Y., Nishiuchi, T., Sato, M., Iwami, M., and Kiya, T. (2013). Visualization of neural activity in insect brains using a conserved immediate early gene, Hr38. Curr. Biol. *23*, 2063–2070.

Hens, K., Feuz, J.-D., Isakova, A., Iagovitina, A., Massouras, A., Bryois, J., Callaerts, P., Celniker, S.E., and Deplancke, B. (2011). Automated protein-DNA interaction screening of Drosophila regulatory elements. Nat. Methods *8*, 1065–1070.

Hens, K., Feuz, J.-D., and Deplancke, B. (2012). A high-throughput gateway-compatible yeast one-hybrid screen to detect protein-DNA interactions. Methods Mol. Biol. *786*, 335–355.

Hyun, S., Lee, Y., Hong, S.T., Bang, S., Paik, D., Kang, J., Shin, J., Lee, J., Jeon, K., Hwang, S., et al. (2005). Drosophila GPCR Han is a receptor for the circadian clock neuropeptide PDF. Neuron *48*, 267–278.

Im, S.H., and Taghert, P.H. (2010). PDF receptor expression reveals direct interactions between circadian oscillators in Drosophila. J. Comp. Neurol. *518*, 1925–1945.

Kadener, S., Stoleru, D., McDonald, M., Nawathean, P., and Rosbash, M. (2007). Clockwork Orange is a transcriptional repressor and a new Drosophila circadian pacemaker component. Genes Dev. *21*, 1675–1686.

Kadener, S., Menet, J.S., Sugino, K., Horwich, M.D., Weissbein, U., Nawathean, P., Vagin, V.V., Zamore, P.D., Nelson, S.B., and Rosbash, M. (2009). A role for microRNAs in the Drosophila circadian clock. Genes Dev. *23*, 2179–2191.

Kaneko, M., and Hall, J.C. (2000). Neuroanatomy of cells expressing clock genes in Drosophila: transgenic manipulation of the period and timeless genes to mark the perikarya of circadian pacemaker neurons and their projections. J. Comp. Neurol. *422*, 66–94.

Kim, E.Y., Bae, K., Ng, F.S., Glossop, N.R.J., Hardin, P.E., and Edery, I. (2002). Drosophila CLOCK protein is under posttranscriptional control and influences light-induced activity. Neuron *34*, 69–81.

Kitayama, Y., Nishiwaki, T., Terauchi, K., and Kondo, T. (2008). Dual KaiC-based oscillations constitute the circadian system of cyanobacteria. Genes Dev. *22*, 1513–1521.

Kuhlman, S.J., Silver, R., Le Sauter, J., Bult-Ito, A., and McMahon, D.G. (2003). Phase resetting light pulses induce Per1 and persistent spike activity in a sub-population of biological clock neurons. J. Neurosci. *23*, 1441–1450.

Kula-Eversole, E., Nagoshi, E., Shang, Y., Rodriguez, J., Allada, R., and Rosbash, M. (2010). Surprising gene expression patterns within and between PDF-containing circadian neurons in Drosophila. Proc. Natl. Acad. Sci. USA *107*, 13497–13502.

Lear, B.C., Merrill, C.E., Lin, J.M., Schroeder, A., Zhang, L., and Allada, R. (2005). A G protein-coupled receptor, groom-of-PDF, is required for PDF neuron action in circadian behavior. Neuron *48*, 221–227.

Lee, C., Bae, K., and Edery, I. (1998). The Drosophila CLOCK protein undergoes daily rhythms in abundance, phosphorylation, and interactions with the PER-TIM complex. Neuron *21*, 857–867.

Lerner, I., Bartok, O., Wolfson, V., Menet, J.S., Weissbein, U., Afik, S., Haimovich, D., Gafni, C., Friedman, N., Rosbash, M., and Kadener, S. (2015). Clk post-transcriptional control denoises circadian transcription both temporally and spatially. Nat. Commun. *6*, 7056.

Li, Y., Guo, F., Shen, J., and Rosbash, M. (2014). PDF and cAMP enhance PER stability in Drosophila clock neurons. Proc. Natl. Acad. Sci. USA *111*, E1284–E1290.

Liang, X., Holy, T.E., and Taghert, P.H. (2016). Synchronous Drosophila circadian pacemakers display nonsynchronous Ca^{2+} rhythms in vivo. Science *351*, 976–981.

Lim, C., and Allada, R. (2013). Emerging roles for post-transcriptional regulation in circadian clocks. Nat. Neurosci. *16*, 1544–1550.

Lin, Y., Stormo, G.D., and Taghert, P.H. (2004). The neuropeptide pigment-dispersing factor coordinates pacemaker interactions in the Drosophila circadian system. J. Neurosci. *24*, 7951–7957.

Maywood, E.S., Reddy, A.B., Wong, G.K.Y., O'Neill, J.S., O'Brien, J.A., McMahon, D.G., Harmar, A.J., Okamura, H., and Hastings, M.H. (2006). Synchronization and maintenance of timekeeping in suprachiasmatic circadian clock cells by neuropeptidergic signaling. Curr. Biol. *16*, 599–605.

McDonald, M.J., and Rosbash, M. (2001). Microarray analysis and organization of circadian gene expression in Drosophila. Cell *107*, 567–578.

Mertens, I., Vandingenen, A., Johnson, E.C., Shafer, O.T., Li, W., Trigg, J.S., De Loof, A., Schoofs, L., and Taghert, P.H. (2005). PDF receptor signaling in Drosophila contributes to both circadian and geotactic behaviors. Neuron *48*, 213–219.

Nagoshi, E., Saini, C., Bauer, C., Laroche, T., Naef, F., and Schibler, U. (2004). Circadian gene expression in individual fibroblasts: cell-autonomous and self-sustained oscillators pass time to daughter cells. Cell *119*, 693–705.

Nagoshi, E., Sugino, K., Kula, E., Okazaki, E., Tachibana, T., Nelson, S., and Rosbash, M. (2010). Dissecting differential gene expression within the circadian neuronal circuit of Drosophila. Nat. Neurosci. *13*, 60–68.

Nitabach, M.N., Blau, J., and Holmes, T.C. (2002). Electrical silencing of Drosophila pacemaker neurons stops the free-running circadian clock. Cell *109*, 485–495.

Nitabach, M.N., Sheeba, V., Vera, D.A., Blau, J., and Holmes, T.C. (2005). Membrane electrical excitability is necessary for the free-running larval Drosophila circadian clock. J. Neurobiol. *62*, 1–13.

Nitabach, M.N., Wu, Y., Sheeba, V., Lemon, W.C., Strumbos, J., Zelensky, P.K., White, B.H., and Holmes, T.C. (2006). Electrical hyperexcitation of lateral ventral pacemaker neurons desynchronizes downstream circadian oscillators in the fly circadian circuit and induces multiple behavioral periods. J. Neurosci. *26*, 479–489.

Park, J.H., Helfrich-Förster, C., Lee, G., Liu, L., Rosbash, M., and Hall, J.C. (2000). Differential regulation of circadian pacemaker output by separate clock genes in Drosophila. Proc. Natl. Acad. Sci. USA *97*, 3608–3613.

Peng, Y., Stoleru, D., Levine, J.D., Hall, J.C., and Rosbash, M. (2003). Drosophila free-running rhythms require intercellular communication. PLoS Biol. *1*, E13.

Perkins, L.A., Holderbaum, L., Tao, R., Hu, Y., Sopko, R., McCall, K., Yang-Zhou, D., Flockhart, I., Binari, R., Shim, H.S., et al. (2015). The transgenic RNAi project at Harvard medical school: Resources and validation. Genetics *201*, 843–852.

Quintero, J.E., Kuhlman, S.J., and McMahon, D.G. (2003). The biological clock nucleus: a multiphasic oscillator network regulated by light. J. Neurosci. *23*, 8070–8076.

Renn, S.C., Park, J.H., Rosbash, M., Hall, J.C., and Taghert, P.H. (1999). A pdf neuropeptide gene mutation and ablation of PDF neurons each cause severe abnormalities of behavioral circadian rhythms in Drosophila. Cell *99*, 791–802.

Roberts, L., Leise, T.L., Noguchi, T., Galschiodt, A.M., Houl, J.H., Welsh, D.K., and Holmes, T.C. (2015). Light evokes rapid circadian network oscillator desynchrony followed by gradual phase retuning of synchrony. Curr. Biol. *25*, 858–867.

Rosbash, M., Bradley, S., Kadener, S., Li, Y., Luo, W., Menet, J.S., Nagoshi, E., Palm, K., Schoer, R., Shang, Y., and Tang, C.H. (2007). Transcriptional feedback and definition of the circadian pacemaker in Drosophila and animals. Cold Spring Harb. Symp. Quant. Biol. *72*, 75–83.

Rosenzweig, M., Brennan, K.M., Tayler, T.D., Phelps, P.O., Patapoutian, A., and Garrity, P.A. (2005). The Drosophila ortholog of vertebrate TRPA1 regulates thermotaxis. Genes Dev. *19*, 419–424.

Sathyanarayanan, S., Zheng, X., Xiao, R., and Sehgal, A. (2004). Posttranslational regulation of Drosophila PERIOD protein by protein phosphatase 2A. Cell *116*, 603–615.

Sehadova, H., Glaser, F.T., Gentile, C., Simoni, A., Giesecke, A., Albert, J.T., and Stanewsky, R. (2009). Temperature entrainment of Drosophila's circadian clock involves the gene nocte and signaling from peripheral sensory tissues to the brain. Neuron *64*, 251–266.

Sellix, M.T., Currie, J., Menaker, M., and Wijnen, H. (2010). Fluorescence/luminescence circadian imaging of complex tissues at single-cell resolution. J. Biol. Rhythms *25*, 228–232.

Seluzicki, A., Flourakis, M., Kula-Eversole, E., Zhang, L., Kilman, V., and Allada, R. (2014). Dual PDF signaling pathways reset clocks via TIMELESS and acutely excite target neurons to control circadian behavior. PLoS Biol. *12*, e1001810.

Shafer, O.T., and Yao, Z. (2014). Pigment-dispersing factor signaling and circadian rhythms in insect locomotor activity. Curr. Opin. Insect Sci. *1*, 73–80.

Shafer, O.T., Kim, D.J., Dunbar-Yaffe, R., Nikolaev, V.O., Lohse, M.J., and Taghert, P.H. (2008). Widespread receptivity to neuropeptide PDF throughout the neuronal circadian clock network of Drosophila revealed by real-time cyclic AMP imaging. Neuron 58, 223–237.

Sivachenko, A., Li, Y., Abruzzi, K.C., and Rosbash, M. (2013). The transcription factor Mef2 links the Drosophila core clock to Fas2, neuronal morphology, and circadian behavior. Neuron 79, 281–292.

So, W.V., and Rosbash, M. (1997). Post-transcriptional regulation contributes to Drosophila clock gene mRNA cycling. EMBO J. 16, 7146–7155.

Stanewsky, R., Lynch, K.S., Brandes, C., and Hall, J.C. (2002). Mapping of elements involved in regulating normal temporal period and timeless RNA expression patterns in Drosophila melanogaster. J. Biol. Rhythms 17, 293–306.

Takahashi, J.S., Ko, C.H., Yamada, Y.R., Welsh, D.K., Buhr, E.D., Liu, A.C., Zhang, E.E., Ralph, M.R., Kay, S.a., and Forger, D.B. (2010). Emergence of noise-induced oscillations in the central circadian pacemaker. PLoS Biol. 8, e1000513.

Tang, C.H., Hinteregger, E., Shang, Y., and Rosbash, M. (2010). Light-mediated TIM degradation within Drosophila pacemaker neurons (s-LNvs) is neither necessary nor sufficient for delay zone phase shifts. Neuron 66, 378–385.

Weiss, R., Bartok, O., Mezan, S., Malka, Y., and Kadener, S. (2014). Synergistic interactions between the molecular and neuronal circadian networks drive robust behavioral circadian rhythms in Drosophila melanogaster. PLoS Genet. 10, e1004252.

Welsh, D.K., Yoo, S.-H., Liu, A.C., Takahashi, J.S., and Kay, S.A. (2004). Bioluminescence imaging of individual fibroblasts reveals persistent, independently phased circadian rhythms of clock gene expression. Curr. Biol. 14, 2289–2295.

Wu, Y., Cao, G., and Nitabach, M.N. (2008). Electrical silencing of PDF neurons advances the phase of non-PDF clock neurons in Drosophila. J. Biol. Rhythms 23, 117–128.

Yao, Z., and Shafer, O.T. (2014). The Drosophila circadian clock is a variably coupled network of multiple peptidergic units. Science 343, 1516–1520.

Yu, W., Zheng, H., Price, J.L., and Hardin, P.E. (2009). DOUBLETIME plays a noncatalytic role to mediate CLOCK phosphorylation and repress CLOCK-dependent transcription within the Drosophila circadian clock. Mol. Cell. Biol. 29, 1452–1458.

Zhao, J., Kilman, V.L., Keegan, K.P., Peng, Y., Emery, P., Rosbash, M., and Allada, R. (2003). Drosophila clock can generate ectopic circadian clocks. Cell 113, 755–766.

Zheng, X., and Sehgal, A. (2008). Probing the relative importance of molecular oscillations in the circadian clock. Genetics 178, 1147–1155.

Supplemental Information

PDF Signaling Is an Integral Part of the _Drosophila_

Circadian Molecular Oscillator

Shaul Mezan, Jean Daniel Feuz, Bart Deplancke, and Sebastian Kadener

Supplemental legends:

Figure S1: Related to Figure 1. The *tim*Tomato reporter construct responds to CLK activity in S2 cells and manifests circadian-like oscillations *in-vivo*. A. Schematic representation of the cloning strategy used to generate the *tim*Tomato reporter construct. Briefly, a cassette containing pCaSpeR4 MCS flanking the *Drosophila* codon optimized Tomato-NLS-PEST CDS with SV40 3'-UTR was inserted into pCaSpeR4 MCS between XhoI and KpnI sites (Red). This resulted in the reconstitution of the MCS and allowed subsequent insertion of *Timeless* promoter and 5'-UTR between XhoI and AvrII sites (Red and Green). Other restriction sites flank the different transcribed regions (i.e. Fluorophore, NLS, PEST and 3'-UTR) thus allowing modularity of these features. **B.** CLK expression in S2 cells activates transcription from the *tim*Tomato reporter. Top: comparison between features of the *tim*Tomato and *tim*YFP constructs. Bottom: Representative pictures of S2 cells transfected with CLK expressed under constitutive (pActin-CLK) or inducible metallothionine promoter (1mM Cu^{2+} pMT-CLK). The low TOMATO signal relative to YFP signal (per cell) is possibly due to the high turnover rate of the PEST. Signal intensity in control wells (No treatment and 0 uM Cu^{+2}) demonstrate the specificity of the 6.4 kb *tim* promoter relative to the leaky 0.7 kb promoter. **C.** Western blot (WB) analysis showing *in-vivo* oscillations of TOMATO in transgenic fly heads. 8 transgenic lines were generated using random insertion of the transgene to the genome. The lines were screened by WB analysis for oscillations in TOMATO, TIM and VRI. At least five lines (i.e. 3, 5, 6, 7, 8) display oscillations in TOMATO signal.

Figure S2: Related to Figure 1. The *tim*Tomato reporter manifests oscillations in transcription in the circadian neurons with phase and amplitude similar to the *timeless* gene products. A. The *tim*Tomato reporter (Red) allows visualization of all neuronal subgroups in the circadian system with high specificity, and does not require immunostaining. **B.** TOMATO signal (red) is co-localized with signal from anti-PDF immunostaining (green) to the *pdf*-expressing cells. **C.** Real-time PCR shows mRNA levels of *tim* and *vri* normalized to *tubulin* across the day in *tim*Tomato fly heads. Error bars represent standard deviation (S.D) of three biological repeats. **D.** A representative picture of a gel from WB analysis that shows the levels of TIM, VRI and TUBULIN in *tim*Tomato fly heads throughout the day from three biological repeats. **E.** Neuronal oscillations in TOMATO. The signal of endogenous TOMATO (red) and GFP (green) in the LNds (Right) and DNs (Left) of UAS-mcd8GFP; *tim*Tomato/*pdf*GAL4 fly brains collected and dissected at the indicated time. Flies were entrained for 3

days in 12:12 Light:Dark (LD) conditions, collected and dissected at the indicated time-points. **F**. Oscillations in TOMATO in brains of reporter flies kept for 3 days under free running conditions (DD3). Top: Representative pictures of brains of *tim*Tomato flies that were dissected at the indicated time in DD3. Bottom: Quantification of the TOMATO signal from the whole brain. Error bars represent S.D of three biological repeats. **G**. Activation of CLKGR in circadian neurons by dexamethasone (Dex) induces TOMATO expression. Representative picture of transgenic *tim*GAL4/*tim*Tomato;UAS-CLKGR (*tim*CLKGR-*tim*Tomato) brains. Flies were grown on vehicle (45% cyclodextrin, Left) or Dex (2.5 mM, Right) containing food under 12:12 h light:dark (LD) conditions for 96h. Brains were dissected at ZT19 and visualized for TOMATO signal (red)**. H**. Representative picture of TOMATO signal in *tim*Tomato/ClkW.T (Left) and *tim*Tomato/CLKSV40 brain (Right), dissected at ZT7. **I**. Oscillations of VRI in the LNds and DNs of cultured brains. Whole mount immunohistochemistry performed on dissected Cantonese S. (CS) brains post-culture. Brains were incubated under 12:12h LD conditions for four days and then collected and stained for VRI (Green) to assess oscillations during the 5th day in culture.

Figure S3: Related to Figure 2. The *tim*Tomato reporter follows dynamics in CLK-driven transcription in ex-vivo culture in real-time and at a single cell resolution. *tim*GAL4/*tim*Tomato; UAS-CLKGR fly brains (*tim*CLKGR-*tim*Tomato) show constant elevation in TOMATO signal in all circadian neuronal groups. Cultured brains were stimulated with Dex and immediately imaged. Left: Single cell quantification of the response and the average signal per group (Error bars represent S.D of the single cell measurements). Right: Snap shots of starting (zero h) and end (96h) point positions of representative brains. Single cell ROIs determined for the quantification of TOMATO signal during the time-lapse imaging (1 frame/30min) are shown in colored circle. **A**. LNvs **B**. LNds **C**. DN1s and DN3s.

Figure S4: Related to Figure 2. Activation of CLK transcriptional activity in the LNvs promotes down regulation in CLK-driven transcription in the rest of the network A. Frequency plots of the number of TOMATO positive cells per neuronal subgroup of cultured *pdf*'CLKGR-*tim*Tomato brains (Based on the same samples and genotype indicated in Figure 2A). Statistical significant was determined for the difference in distributions between vehicle and Dex-treated brains using two-sample Kolmogorov-Smirnov test (K-S test). NS=not significant, * p< 0.05 ** p<0.01, *** p<0.001 ****

2

p<0.0001. **B.** Dexamethasone (Dex) was applied on control *tim*Tomato;UAS-CLKGR (CLKGR-*tim*Tomato) cultured brains. The kinetic of the response was monitored by time-elapsed imaging (1 frame / 40min). The quantification shows that this does not stimulates any change in TOMATO signal in the different neuronal groups indicated. **C.** Comparison of the quantification of TOMATO signal based on the number of cell detected in the same samples of brains indicated in Figures 2A and 2B, and that were cultured under vehicle conditions only.

Figure S5: Related to Figure 3. CLK regulates *pdf* expression. **A.** *Ex-vivo* activation of CLK-dependent transcription by Dex in the LNvs of *pdf*GAL4/*tim*Tomato;UAS-CLKGR (*pdf*CLKGR), leads to increased PDF levels at ZT19 as measured by immune-staining (Green). Left: Representative pictures of vehicle (Top) and Dex (Bottom) treated brains. Right: Quantifications of the response using intensity (Top) and cell number count (Bottom). N_{Dex}=39, $N_{vehicle}$=37 hemispheres. **B.** Expression of *Clk* RNAi reduces PDF expression. Brains were immune-labeled with anti-PDF (Purple) at ZT5. Top: representative pictures of *pdf*Tomato/CLK^{RNAi} brains (CLK^{RNAi}) (Left) and *pdf*GAL4;*pdf*Tomato/CLK^{RNAi} (*pdf*GAL4;CLK^{RNAi}) (Right). Bottom: quantification of PDF expression in the LNvs of the same samples analyzed in Figure 3B. N=24, 25 hemispheres respectively. Statistical significance was determined using two tail Student's T-test, NS=not significant * $p < 0.05$ ** $p<0.01$, *** $p<0.001$ **** $p<0.0001$. Error bars represent SEM. **C.** Left: Scheme of the *pdf*Tomato transcriptional reporter. Sizes of the different modules are written above. Restriction sites are indicated below the scheme. NLS: Nuclear Localization Signal; PEST: mouse ornithine decarboxylase; SV40-3'-UTR: Simian Virus 3' Untranslated Region. Right: Representative picture demonstrating the specificity of the reporter.

Figure S6: Related to Figure 4 and Table 1. Identification of putative regulators of *pdf* using Yeast One Hybrid (Y1H). Schematic representation of the fragments of the *pdf* control region that were generated in order to identify putative regulators using a yeast one hybrid (Y1H) screen. The screen identified interaction with 27 genes (Table 1). Interestingly, 4 of these genes are CLK targets and enriched in the LNvs, and they interact with *pdf* most proximal promoter fragment generated. Two of these genes are also Mef2 direct targets - Hr38 and SR.

3

Figure S7: Related to Figure 4. Neuronal Activity and the activity regulated genes - *Hr38* and *sr* - regulate *pdf* expression. (A-C) *Pdf*GAL4 and *tim*GAL4 flies containing a UAS-dicer2 transgene (*pdf*GAL4, dcr2) were crossed *dhr38* and *sr* RNAi lines. PDF immuno-labeling (green) was performed at ZT5 on brains carrying different genotypes as indicated in the figure. Shown are representative pictures (Top) and quantifications (Bottom). **A.** Expression of *hr38*^RNAi transgene in the *pdf*-expressing cells causes large reduction in PDF levels (N=27, 22, 30 hemispheres respectively). **B.** Expression of *hr38*^RNAi transgene in clock cells using the *tim*GAL4 driver causes large reduction in PDF levels (N=27, 22, 23 hemispheres respectively). Control brains of UAS-HR38^RNAi are common to the experiments presented in A and B that were performed together). **C.** Expression of *sr*^RNAi transgene in the *pdf*-expressing cells causes large increase in PDF levels (N=24, 32, 30 hemispheres respectively. **D.** *pdfGAL4;pdf*Tomato/UAS-TrpA1 and *pdf*Tomato/UAS-TrpA1 flies were incubated at 33^0C for 2h. TOMATO (red) and PDF (green). (Based on the same samples and genotype indicated in Figure 4C). Statistical significance was determined using two tail Student's T-test, NS=not significant * $p< 0.05$ ** $p<0.01$, *** $p<0.001$ **** $p<0.0001$. Error bars represent SEM.

Movie S1: Related to Figure 2. Following dynamics in CLK-driven transcription in the LNvs at a single cell resolution using the *tim*Tomato circadian transcriptional reporter.

Movie S2: Related to Figure 2. Following dynamics in CLK-driven transcription in the LNds at a single cell resolution using the *tim*Tomato circadian transcriptional reporter.

Movie S3: Related to Figure 2. Following dynamics in CLK-driven transcription in the DNs at a single cell resolution using the *tim*Tomato circadian transcriptional reporter.

Movie S4: Related to Figure 2. Down-regulation in transcription from the *tim*Tomato in the DNs in response to activation of CLK-driven transcription in the LNvs.

Supplemental Experimental Procedures:

Cloning of reporter constructs and DNA baits of the *pdf* promoter:

To generate the *tim*Tomato reporter construct, a reconstitution cassette (for the pCaSpeR4 MCS) containing a *Drosophila* codon optimized TdTomato-NLSx3-PEST coding sequence with a SV40 3'-UTR (synthesized by GenScript) was cut from pUC57 carrier vector and inserted into pCaSpeR4 between XhoI-KpnI sites (See Figure S1A for details about restriction sites included in the cassette). A previously characterized 6.4 kb fragment containing the promoter and 5'-UTR stretching into to the second exon ATG in the *timeless* gene (Stanewsky et al., 2002) was amplified from genomic DNA using the forward primer (include a XhoI restriction site) 5'-TCCGAACTCGAGTCCAGGTCAACACTGTCATA-'3 and reverse primer (includes a AvrII restriction site) 5'-ACGGTTCCTAGGCGACTGCGAACATTGAGGTA-'3, and ligated between XhoI and AvrII sites in the reconstructed MCS of pCaSpeR4.

To generate the *pdf*Tomato reporter construct a previously characterized (Park et al., 2000) 2.45 kb fragment containing the genomic region upstream to the *pdf* gene transcription start site, was cut from a carrier vector and ligated in a pattB-sv40 based vector between BamHI and EcoRI. *Drosophila* codon optimized TdTomato-NLSx3-PEST coding sequence with a SV40 3'-UTR was cut from pUC57 carrier vector and inserted downstream to the *pdf* promoter in the pattB-sv40 vector between EcoRI and NotI.

To generate DNA baits of the *pdf* promoter for *Drosophila* transcription factor screen (Y1H) we used a carrier vector containing the 2.45 kb promoter of the *pdf* gene as a template to generate five overlapping PCR fragments approximately 600 bp long, that contain restriction sites for BamHI-Acc65I, using the following sets of primers:

For: CGCGGATCCTCCGTGGGTTTCATCCTTAC Rev: CGGGGTACCAGGAGCGTCTTGGTCACATC

For: CGCGGATCCACGAATCATCTTCGGCTTGT Rev: CGGGGTACCCAGTCACACAACGCACATCA

For: CGCGGATCCTGTGGCTGCATGGAAAGTTA Rev: CGGGGTACCCCTCCTCCTCCTCCTCCTC

For: CGCGGATCCTTGGAACCTAGCCCTGATTG Rev: CGGGGTACCATAGCTAGCTCGGCAGTTGG

For: CGCGGATCCCAAGACAATTGGCGGAATTT Rev: CGGGGTACCAGCAGGAGACTTGCGAAT GA

Fragments were cloned into BamHI-KpnI site in a pENTRY-5' vector and then sub-cloned using the recombination based Gateway cloning strategy into pMW2 pBD-HIS using LR Clonase (Invitrogen).

Drosophila **adult brain culture:**

Post-culture applications: Visualization of TOMATO or immune-staining of the brains were performed immediately after fixation to avoid fading of TOMATO signal. For time-course experiments, fixed brains were re-immersed in 0.2% PFA and placed in 4˚C until all samples collected (more than 72h in 4˚C under these conditions will result in high TOMATO background signal in the sample).

Immunofluorescence:

Performed as previously described (Lerner et al., 2015) with minor modifications. 1st antibodies were used at: 1:1500 dilution for mouse Anti-PDF (a gift from the Justin Blau lab), 1:1000 Rat anti-TIM (a gift from Michael Rosbash) and 1:2000 guinea pig anti-VRI (a gift from Paul Hardin). The Anti-mouse, anti-rat and anti-guinea pig 2nd antibodies were diluted 1:1000 (Alexa Fluor conjugated 488, 555 and 633).

qPCR:

Real-time RT-PCR was performed as described in (Weiss et al., 2014), using the same primer sequences for tim and vri. Primers for Drosophila codon optimized Td-Tomato used in this study were: For: 5'-TGGACATCACGTCGCATAAT-'3 and Rev: 5'-TACAGCTCATCCATGCCGTA-'3.

Western Blot analysis:

Western blots with anti-VRI, anti-TIM and anti-TUBULIN antibodies were performed as described in (Weiss et al., 2014). TOMATO was detected by anti-mouse DsRed polyclonal antibody (purchased from Clontech).
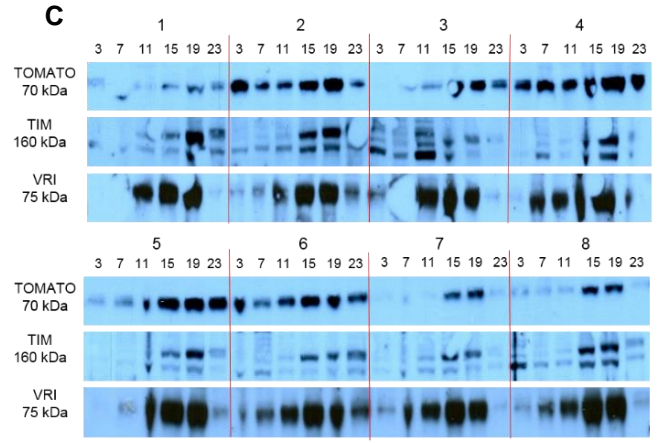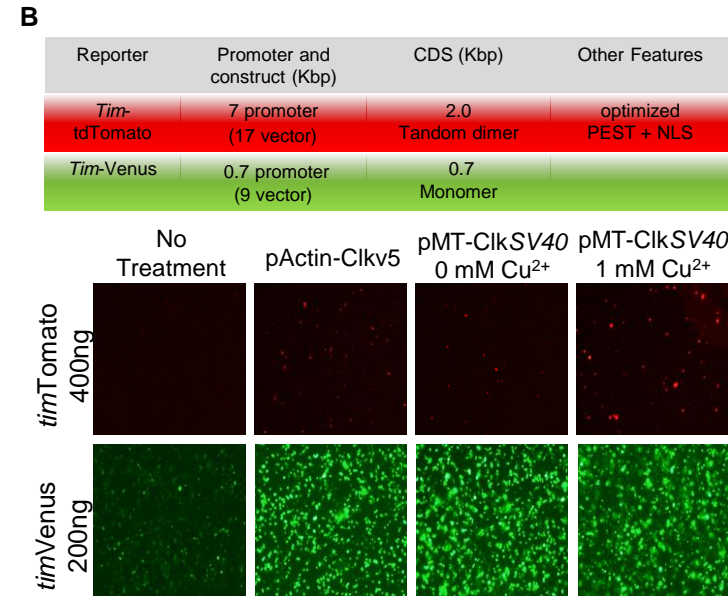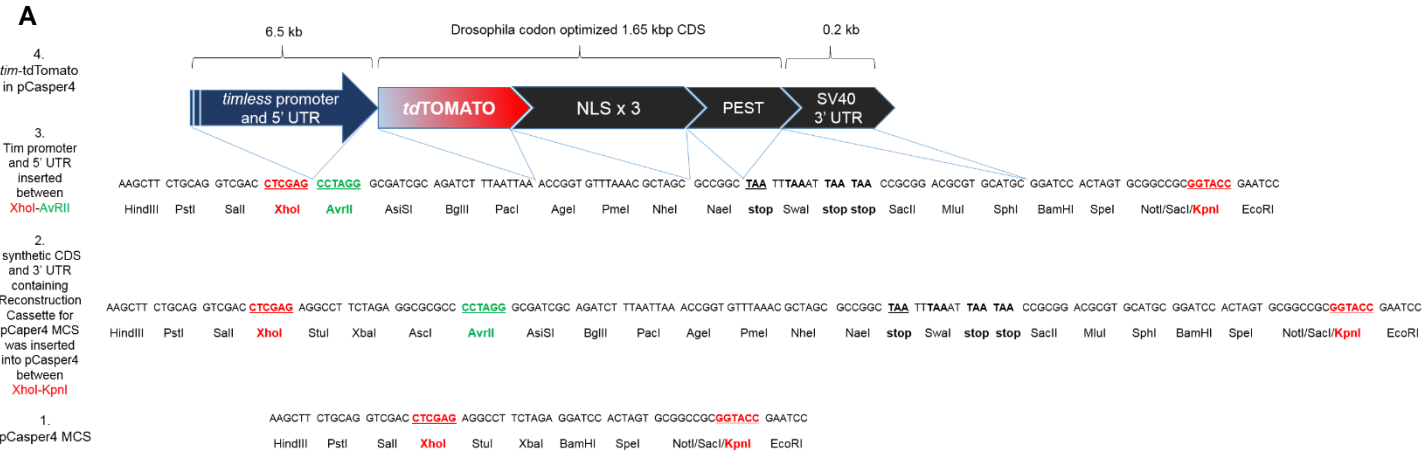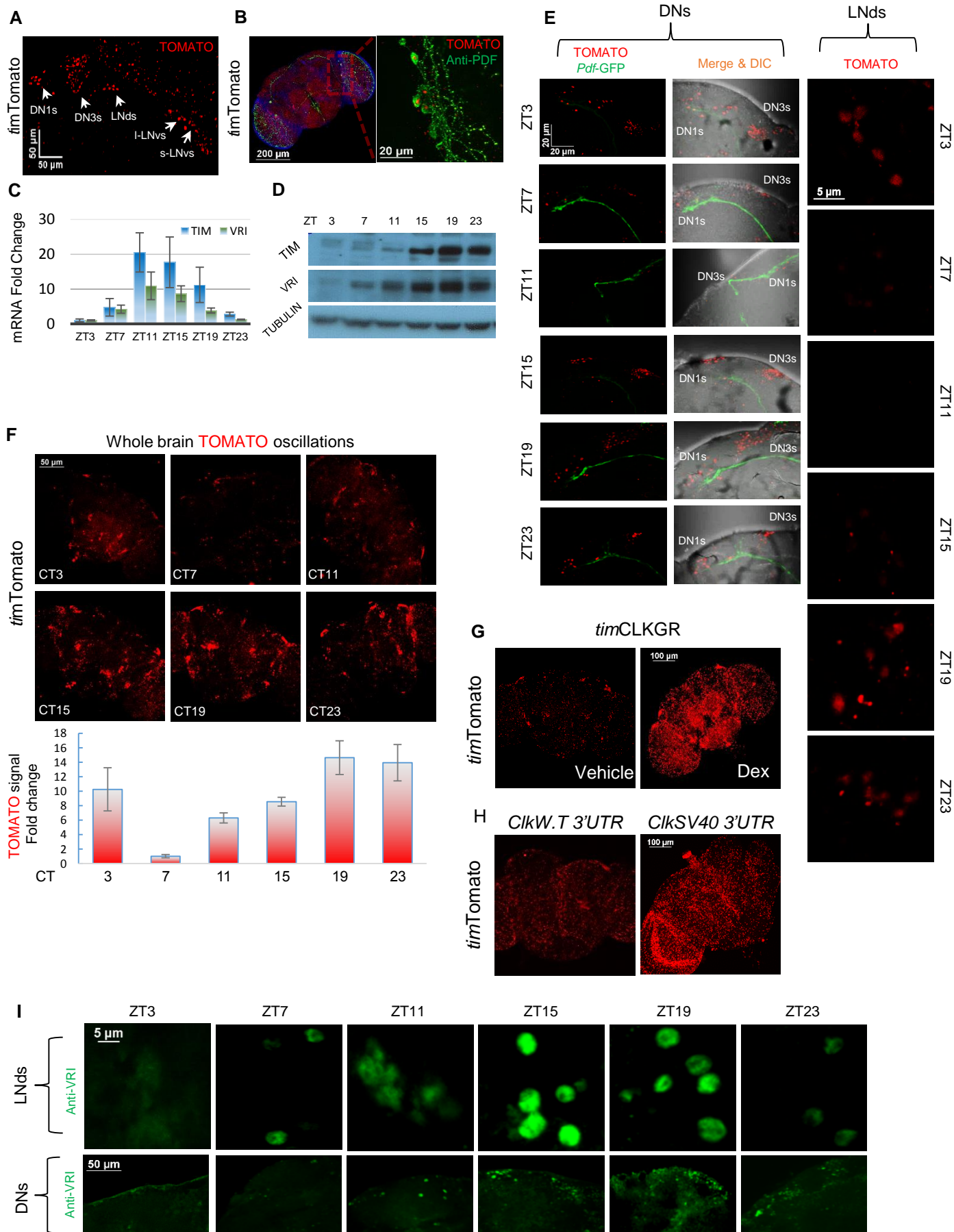
Figure S1

A

4. *tim*-tdTomato in pCasper4

3. Tim promoter and 5' UTR inserted between XhoI-AvrII

2. synthetic CDS and 3' UTR containing Reconstruction Cassette for pCaper4 MCS was inserted into pCasper4 between XhoI-KpnI

1. pCasper4 MCS

6.5 kb — *timless* promoter and 5' UTR

Drosophila codon optimized 1.65 kbp CDS — *td*TOMATO — NLS x 3 — PEST

0.2 kb — SV40 3' UTR

AAGCTT CTGCAG GTCGAC **CTCGAG** **CCTAGG** GCGATCGC AGATCT TTAATTAA ACCGGT GTTTAAAC GCTAGC GCCGGC **TAA** TTTAAAT **TAA TAA** CCGCGG ACGCGT GCATGC GGATCC ACTAGT GCGGCCGC**GGTACC** GAATCC

HindIII PstI SalI **XhoI** **AvrII** AsiSI BglII PacI AgeI PmeI NheI NaeI **stop** SwaI **stop stop** SacII MluI SphI BamHI SpeI NotI/SacI/**KpnI** EcoRI

AAGCTT CTGCAG GTCGAC **CTCGAG** AGGCCT TCTAGA GGCGCGCC **CCTAGG** GCGATCGC AGATCT TTAATTAA ACCGGT GTTTAAAC GCTAGC GCCGGC **TAA** TTTAAAT **TAA TAA** CCGCGG ACGCGT GCATGC GGATCC ACTAGT GCGGCCGC**GGTACC** GAATCC

HindIII PstI SalI **XhoI** StuI XbaI AscI **AvrII** AsiSI BglII PacI AgeI PmeI NheI NaeI **stop** SwaI **stop stop** SacII MluI SphI BamHI SpeI NotI/SacI/**KpnI** EcoRI

AAGCTT CTGCAG GTCGAC **CTCGAG** AGGCCT TCTAGA GGATCC ACTAGT GCGGCCGC**GGTACC** GAATCC

HindIII PstI SalI **XhoI** StuI XbaI BamHI SpeI NotI/SacI/**KpnI** EcoRI

B

Reporter	Promoter and construct (Kbp)	CDS (Kbp)	Other Features
Tim-tdTomato	7 promoter (17 vector)	2.0 Tandom dimer	optimized PEST + NLS
Tim-Venus	0.7 promoter (9 vector)	0.7 Monomer	

No Treatment | pActin-Clkv5 | pMT-Clk*SV40* 0 mM Cu²⁺ | pMT-Clk*SV40* 1 mM Cu²⁺

*tim*Tomato 400ng

*tim*Venus 200ng

C

1   2   3   4
3 7 11 15 19 23   3 7 11 15 19 23   3 7 11 15 19 23   3 7 11 15 19 23

TOMATO 70 kDa
TIM 160 kDa
VRI 75 kDa

5   6   7   8
3 7 11 15 19 23   3 7 11 15 19 23   3 7 11 15 19 23   3 7 11 15 19 23

TOMATO 70 kDa
TIM 160 kDa
VRI 75 kDa

Figure S2

Figure S3

A

s-LNvs ****

LNds **

DN3s ***

l-LNvs *

DN1s **

DN2s NS

Vehicle
Dex

Frequency %

Number of cells (TOMATO signal)

B

uas-CLKGR-*tim*Tomato

Relative Intensity TOMATO signal

Hours post Dex stimulation

l-LNvs DN3s DN1s B.G

C

Average number of cells TOMATO signal

**** NS * NS

pdfClkGR-tim-Tomato
Han5; pdfClkGR-tim-Tomato

s-LNvs DN1 DN3 LNds

Figure S4

A

pdf-CLKGR

Vehicle

25 µm
25 µm

PDF

Dex

**

PDF signal Fold Change Intensity

1.5
1.25
1
0.75
0.5
0.25
0

☐ Vehicle
■ Dex

LNvs cell body

PDF signal Fold Change Average number of cells

2
1.5
1
0.5
0

**   **

☐ Vehicle
■ Dex

s-LNvs   l-LNvs

B

uasCLK ^{RNAi} *pdf*Gal4;uasCLK ^{RNAi}

PDF

pdf-Tomato

20 µm

PDF Signal Relative Intensity

200
150
100
50
0

*   NS

s-LNvs   l-LNvs

■ UAS- CLK RNAi   ■ pdfGal4/UAS- CLK RNAi

C

2.45 kb   *Drosophila* codon optimized 1.65 kb CDS: 0.2 kb

pdf promoter

*td*TOMATO   NLS x3   PEST   SV40 3' UTR

BamHI   AvrII   AgeI   NaeI   MluI SacII   BamHI NotI

4 l-LNvs   4 s-LNvs

TOMATO

Figure S5

Figure S7